International Journal of Nanoelectronics and Materials
*Volume 11, No. 4, Oct 2018* [419-426]

# Structural, Dielectric and Electric Properties of Manganese-Doped Barium Titanate

Suravi Islam[1]*, Ayesha Siddika[2], Nazia Khatun[1], Mohammad Sajjad Hossain[1], Most Hosney Ara Begum[1] and Nurzamn Ara Ahmed[1]

[1]*Industrial Physics Division, BCSIR Laboratories, Dhaka.*
[2]*Institute of Fuel Research and Development (IFRD), Bangladesh Council of Scientific and Industrial Research (BCSIR), Dr. Kudrat-i-Khuda Road, Dhaka-1205, Bangladesh.*

Received 7 January 2018; Revised 21 June 2018; Accepted 27 June 2018

**ABSTRACT**

*The Dielectric, Electric Properties and Microstructure of Ba $Mn_x Ti_{1-x} O_3$ (where x = 0.0, 0.01, 0.02, 0.03, 0.04) ceramics have been investigated. The ceramic samples were prepared by Solid-State Reaction Method. The SEM microstructure shows grain size decreased from 192.93 nm down to 167.05 nm. Tetragonal structure was found for samples 0.03% and 0.04% Mn-doped $BaTiO_3$ while others showed pseudo-cubic structure. The Dielectric Constant measurements were executed as a function of temperature. Pure and 0.03% Mn-doped ceramics showed improved dielectric constant around Curie temperature region. The temperature dependence of electrical resistivity for all samples were noted acquired that the resistivity changes with the addition of $Mn^{+3}$ ions in the conduction process accordingly, except pure barium titanate i.e, x=0.0.*

**Keywords:** Pervoskite, Tetragonality, Polarization, Dielectric Property.

## 1. INTRODUCTION

Barium Titanate (BT) is a ferroelectric material with perovskite structure which has been of practical importance for over 60 years due to its electrical properties [1]. It is used in multilayer capacitors as dielectric material, piezoelectric transducers, gas sensors, thermistors and so on. The crystal structure is a primitive cube, with the Ba larger cation in the corner, the Ti smaller cation in the middle of the cube and oxygen in the centre of the faces edges [2]. The ferroelectric properties are connected with a series of three structural phase transitions. The sequences of the phases upon heating are rhombohedral, orthorhombic, tetragonal, cubic. The most generaly methods used for the synthesis of $BaTiO_3$ are solid-state reaction [3], mechanochemical synthesis [4] and wet chemical methods such as sol-gel (A. Kareiva *et al*.), hydrothermal (Song Wei Lu *et al*.), co-precipitation method (Paolo Nanni *et al*.). The synthesis method has a considerable consequence on the expected characteristics [2] [5] [6] [7]. The high energy ball milling using high density milling media like tungsten carbide produced very fine impurity free tetragonal BT nanoparticles. The particle size is found reduced than the conventional heating other microwave heated samples. The dielectric loss was also comparatively less for microwave heated samples [8]. W. Cai *et al*. prepared Mg-doped $BaTiO_3$ by conventional solid state reaction method and found that Mg can suppress grain growth of BTO ceramics [9]. M. M. Vijatovic´ *et al*. showed in their paper on antimony doped barium titanate that cubic barium titanate nanopowders were obtained by the modified Pechini process and the grain size gained with the increment of Sb concentration. The possible reason for dielectric permittivity increase could be

*Corresponding Author: *suravii@yahoo.com*

the existence of small grains in doped samples. Also, reaching the critical grain size could influence further decrease of dielectric permittivity value [10]. Sitko D. *et al*. [11] showed that increasing content of Mn ions in the BT causes gradual diffusion of all the phase transformations and in particular, the PE–FE phase transition. T Hashishin *et al*. the 0.35 mol% Nd-doped $BaTiO_3$ ceramics sintered via three steps heating at 1340°C for 2 h after hydrothermally synthesized at 240°C for 24 h, exhibited high PTCR effect compared with the 0.35 mol% Nd-doped BaTiO3 ceramics sintered by the conventional solid-state process [12]. X. Wang *et al*. explained in their study that, in Mn-doped $BaTiO_3$ there lies valence states consists of $Mn^{+2}$, $Mn^{+3}$ and $Mn^{+4}$. In addition to that Mn is associated with Ti sites and cooperates in the collective motion in the lattice [13]. The purpose of our work is to investigate the dielectric, electric properties and microstructure of manganese doped Barium Titanate $BaTiO_3$.

## 2. MATERIALS AND METHOD

The precursor mixture was obtained by analytical grade $BaCO_3$(99.0%), $TiO_2$(99.0%) and $Mn_2O_3$(99.9%) all from MERCK, Germany. All the raw materials were milled in a high precision planetary ball mill (FRITSCH "PULVERISETTE 6") individually for 5 hours. SEM analysis showed that milling downsized the particle of the material into nanometer range. The grounded $BaCO_3$, $TiO_2$ and $Mn_2O_3$ were mixed together according to the stoichiometric equation $BaMn_xTi_{1-x}O_3$ where x= 0, 0.01, 0.02, 0.03, 0.04. After that, each mixture was milled for 18 hours in dry medium again using aluminum ball to avoid contamination. The mixtures were pre sintered at 700˚C for 3 hours in air. The ground BT was mixed with a binder (4% of Polyvinyl alcohol aqueous solution) and were pressed into disk-like pellets applying pressure 2±0.5 M Pa for 1 min. The pellets were then sintered in a programmable muffle furnace (Nabertherm) at 1150˚C for 3 h in the air. The synthesized samples were characterized by SEM (Hitachi, S-3400N), XRD (EMMA, GBC Scientific equipment radiation functioned at 40KV and 40 mA, source Cu-kα (λ=1.54052°A) and Impedance Analyzer (Agilent 4294A, 40 kHz to 120MHz).

## 3. RESULT AND DISCUSSION

### 3.1 Structural Property

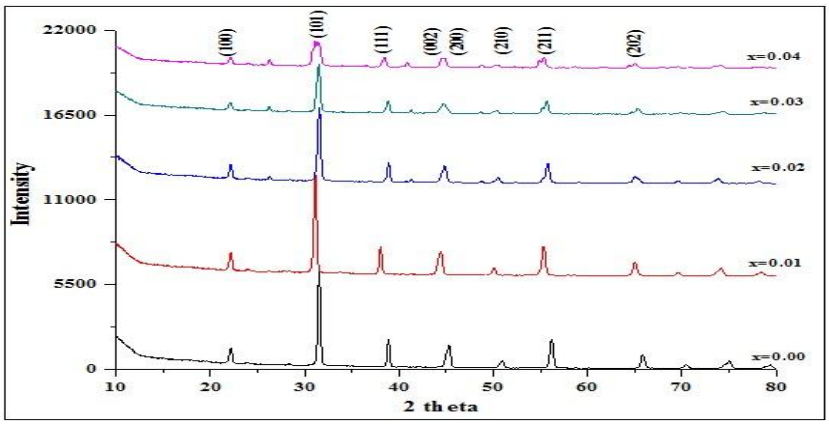


**Figure 1.** XRD Patterns of $BaMn_xTi_{1-x}O_3$.

X-ray diffraction patterns of different samples doped and undoped with different composition of $Mn_2O_3$ content of 0.01%, 0.02%, 0.03% and 0.04% respectively. Tetragonality increases with the doping content. Pure and 0.01 and 0.02% Mn-doped $BaTiO_3$ shows pseudo-cubic structure,

while 0.03% and 0.04% doped $BaTiO_3$ shows a tetragonal structure having a slightly increasing c/a ratio of 1.004648 and 1.000548 respectively.

### 3.2. Microstructure Analysis

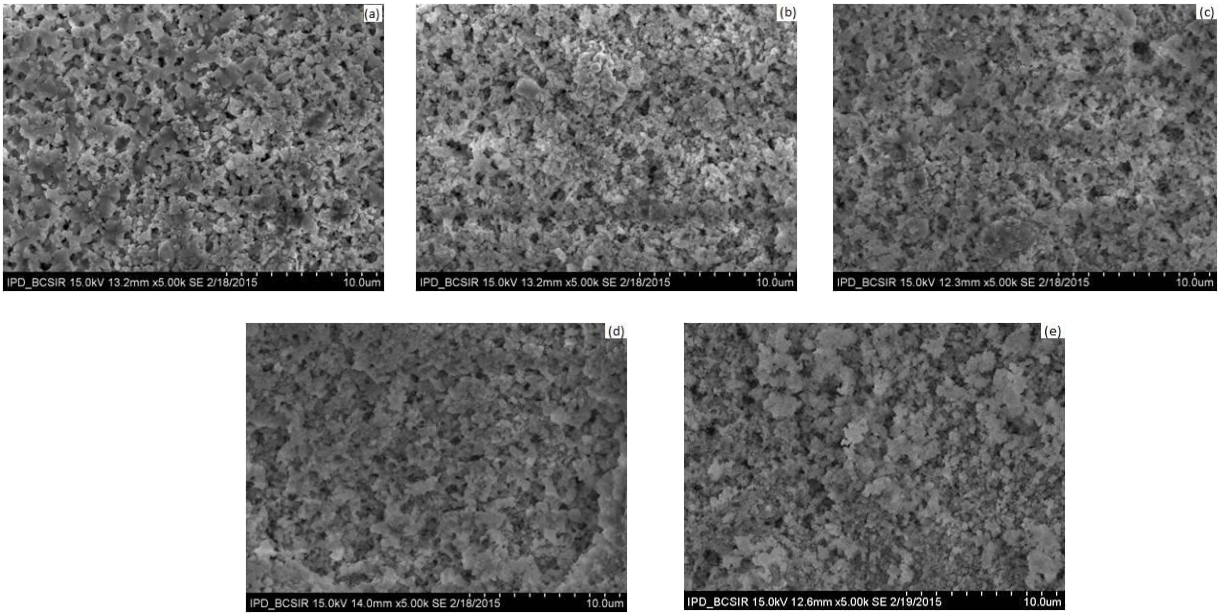


**Figure 2.** SEM micrographs of pure and doped $BaTiO_3$.

The SEM study (figure 2) implemented on both pure and Mn-doped BT. Microstructures show agglomerated grain distribution throughout the sample. The SEM micrographs examined that the average grain size of Mn-doped $BaTiO_3$ ceramics are 183.2 nm, 167.05 nm, 192.93 nm, 178.52 nm, 173.46 nm as the Mn content increases from 0, 0.01, 0.02, 0.03, 0.04% respectively. It is clear that the mixture of Manganese does not affect radically on the average grain size of BTO ceramics. From the figure, it can be analyzed that BT becomes less porous and with the increase of Mn content.

### 3.3. Dielectric Properties

Ferroelectric materials have high dielectric constant [14]. Dielectric properties of the ceramics can be described by the temperature dependence of the dielectric constant and dielectric loss (Table 1. and figure 3(a)) in the heating process. Table 1 shows the change of dielectric constant with temperature. In the case of ferroelectric ceramics, the dielectric maxima at the temperatures which is called the Curie temperature are corresponds to the structural phase transition, i.e, a ferroelectric to a paraelectric transition [15]. The dielectric constant was calculated from the capacitance using the following equation,

$$\varepsilon = \frac{Cd}{\varepsilon_0 A} \tag{1}$$

where C is the capacitance (F), d the thickness (m), A is the area ($m^2$) and $\varepsilon_0 = 8.85 \times 10^{-12}$ F $m^{-1}$.
Table1 shows that the transition temperature $T_c$ was found 120°C for pure and 130°C for 0.01, 0.02 and 0.04% Mn composition and 135°C for 0.03% Mn composition. Structural disorder might be the reason for the shift of $T_c$[16]. The dielectric constant of the sample shows the same characteristics. Table 1 gives a data showing how dielectric constant changes with varying manganese doping. The maximum dielectric constant was found 43800 while Ni-doped BT showed a maximum value in the dielectric constant is 81200 at the transition temperature; this

is one of the highest values reached for ceramic capacitors [17]. The energy storage aptitude i.e, dielectric constant of a capacitor can be improved by using dielectric materials. Reason behind the improved dielectric constant is induced charges created due to dielectric polarization, increase charges on the plates of the capacitor. The dielectric constant ε of a material is

$$\varepsilon = \varepsilon_0 + \frac{P}{E} \quad (2)$$

Where, $\varepsilon_0$ is the dielectric constant in vacuum, P is the polarization and E is the electric field intensity [18]. Below Curie temperature, polarization of a material without any applied external electric field on it is known as spontaneous polarization, i.e, random orientation of the electric dipoles. A relation lies between the spontaneous polarization and the crystal structure of a ferroelectric material. As a result of the decrement of the crystallinity of a material, ferroelectricity refrains and amorphous state created [19]. From Table 1, maximum dielectric constant with varying temperature was found for the minimum grain size. But for the rest of the samples dielectric constant increases with the increasing grain size. This is because of the change of spontaneous polarization of the material. The dielectric constant values of the BT were studied in the frequency range 55 kHz to 110MHz at room temperature is given in figure. The dielectric constant of 0.01% Mn-doped Barium Titanate is found maximum and minimum dielectric constant is found for pure $BaTiO_3$. According to Clausius–Mosotti relation, the dielectric constant of the material is associated to polarizability [20]. At this lower frequency range dielectric constant is found due to orientational, electronic and ionic polarization[21]. Inhomogeneous dielectric structure might be responsible for the large value of the dielectric constant. Impurities, porosity and grain structure resembles the in homogeneities [22].

As shown in figure 3(a), it is clear that the dielectric loss decreases drastically with the increasing Mn contents. Dopants like $Mg^{2+}$, $Ni^{2+}$, $Fe^{3+}$, $Mn^{2+}$, $Mn^{3+}$, $Co^{2+}$, $Co^{3+}$, $Al^{3+}$, $Cr^{3+}$, $Bi^{3+}$ can occupy the B site of the $ABO_3$ perovskite structure, behave as an electron acceptor and decrease the dielectric loss[23]. Maximum Dielectric losses were found 0.017, 0.013, 0.008, 0.009, and 0.008 for pure BT and 0.01, 0.02, 0.03 and 0.04% with Mn additives respectively.

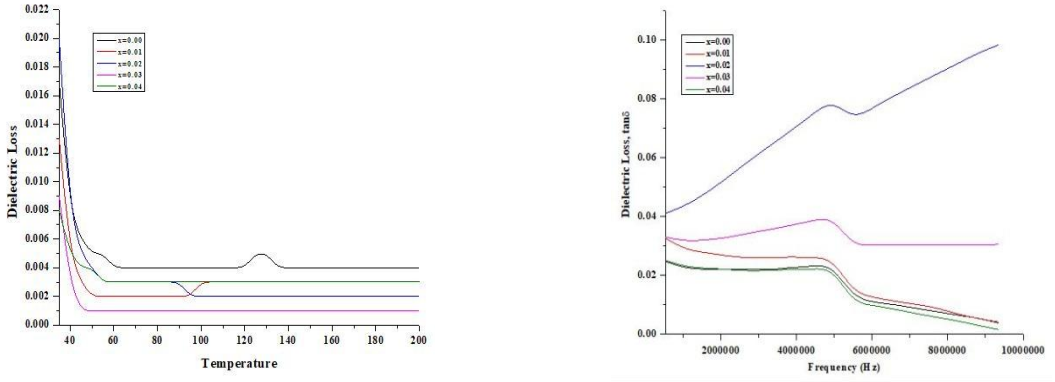


(a) (b)

**Figure 3.** Variation of Dielectric Loss as a function of (a) Temperature and (b) Frequency for various Ba $Mn_xTi_{1-x}O_3$.

From figure 3(b), the tangent loss with frequency was also found increased with the Mn concentration, except for x=0.04. But for 0.04% Mn additive value, the dielectric constant was found low. However, the value of the loss factor was increased with the increasing frequency. The combined effect of space charge polarization and domain wall relaxation causes a tangent loss in ferroelectrics [21].

**Table 1** Dielectric Constant and Curie temperature variation of $BaMn_xTi_{1-x}O_3$

| Value of x for sample Composition | Temperature Dependent Dielectric Constant | Curie Temperature (Tc)°C | Frequency Dependent Dielectric Constant |
|---|---|---|---|
| 0.00 | 37700 | 120 | 326.3791 |
| 0.01 | 43800 | 130 | 898.0966 |
| 0.02 | 40900 | 130 | 1680.389 |
| 0.03 | 38400 | 135 | 358.0475 |
| 0.04 | 36300 | 130 | 417.013 |

## 3.4.Electric Property

In doped BT, the temperature-dependent resistivity was found. It is a grain boundary dependent characteristics [24]. To calculate resistivity we use the following equation,

$$R = \rho \frac{L}{A} \quad (3)$$

Where A is the cross-sectional area of the sample and L is the length separating the contacts.

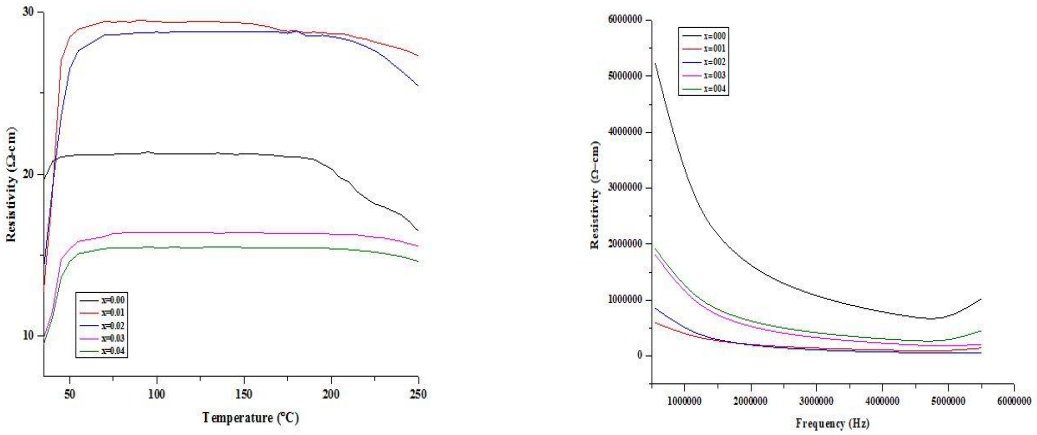


(a) (b)

**Figure 4.** Variation of resistivity as a function of (a) Temperature and (b) Frequency of $BaMn_xTi_{1x}O_{3.}$

### *3.4.1.Temperature-dependent Resistivity*

The temperature-dependent electrical resistivity of the samples was measured by using two probe techniques. This graphical expression (figure 4(a)) shows BT with 0.01% Mn doping exhibit the highest PTRC behavior whereas with 0.02% and 0.04% Mn-doping, the resistivity curves collapse. In our previous study, we have seen that Bi-doped BT has low PTRC behavior [25] also dielectric constant and resistivity depends on the grain size [26] for Ce and Zr-doped BT. The potential barrier, positioned at the grain boundary and entrapping of the charge carriers through the polar region increases the resistivity [11].

### 3.4.2. *Frequency Dependent Resistivity*

Frequency dependent electrical resistivity is shown in the figure 4(b). Graphs show that BT with 0.03% and 0.04% Mn-doping exhibit higher resistivity. So resistivity increases with the doping

concentration. From figure it can also be assumed that resistivity is lower in the MHz frequency range, i.e. in this range conductivity is higher. The frequency dependent conductivity can be explained by the jump relaxation model, where the translational hopping and localized orientational hopping are accountable for electron conduction. At low frequency, the conductivity may be due to the translational hopping and at higher frequencies, the conductivity may be due to the localized orientation hopping [27].

## 4. CONCLUSION

The polycrystalline samples of Ba $Mn_x Ti_{1-x} O_3$ (x=0.0 - 0.04) were prepared by conventional solid-state reaction route. The XRD analysis exposes the presence of both pseudo-cubic and tetragonal phases. The SEM study confirms the microstructure of the samples. Maximum Curie temperature was found $135^0$C. The dielectric measurements have shown that our samples are responsive to the applied frequency and temperature. The samples indicated PTC behavior in resistivity. Highest resistivity was noticed for 0.01% Mn-doped $BaTiO_3$. The frequency dependent resistivity specifies that the conduction is due to localized orientational hopping.

## ACKNOWLEDGEMENTS

The authors gratefully acknowledge Bangladesh Council of Science and Industrial Research (BCSIR) for funding this research work. We would like to express our gratitude to director, BCSIR Laboratories, Dhaka and thanks all the scientists and staff of Industrial Physics Division for their cooperation.

## REFERENCES

[1] P. N. Nikolarakis, I. A. Asimakopoulos & L. Zoumpoulakis, 7023437 (2018) 11.
[2] M. M. Vijatović, J. D. Bobić, B. D. Stojanović**,** Science of Sintering **40** (2008) 155-165.
[3] T. Shiosaki, H. Takeda, R. Goto, T. Kinoshita, T. Shimada & Y. Katsuyama; Applications of ferroelectrics, 2006 ISAF '06 15th IEEE international symposium.
[4] B. D. Stojanovic *et al.* Journal of the European Ceramic Society **25** (2005) 1985–1989
[5] A. Kareiva, S. Tautkus, R. Rapalaviciute, Journal of Material Science **34** (1999) 4853–4857
[6] Song Wei Lu, B. Lee, ZL Wang, WD Samuels, Jour. of Crystal Growth **219** (2000)269-276.
[7] Paolo Nanni, M. Viviani, V. Buscaglia, Handbook of Low and High Dielectric Constant Materials and Their Application; Materials and Processing (1).
[8] S. Thirumalai, B.P. Shanmugavel, Journal of Microwave Power and Electromagnetic Energy, **45**, 3 (2011) 121-127.
[9] W. Cai, C. L. Fu1 & C. X. Zhao, Advance in Applied Ceramics **110**, 3 (2011) 181-185.
[10] M.M. Petrovic´, J.D. Bobic´, J. Banys, B.D Stojanovic´, Materials Research Bulletin **48** (2013) 3766–3772.
[11] Sitko D., Bąk W., Garbarz B., Antonova M. & Jankowska S. I., Ukr. J. Phys. Opt. **13, 3** (2012).
[12] T. Hashishin *et al.* IOP Conf. Ser.: Mater. Sci. Eng. **18** 092031 (2011).
[13] X. Wang, M. Gu, B.Yang, S.ng Zhu, Microelectronic Engineering **66** (2003) 855–859.
[14] R. Rotaru, *et al.* Journal of American Ceramic Society **100**, 137 (2017) 4511- 4518
[15] V. Paunovic, V. Mitic, L. Kocic, Electronics and Energetics **29** 2 (2016) 285-296.
[16] R. Islam, S Chowdhury, S. N. Rahman, Md. J. Rahman **13**, 3 (2012) 248-251.
[17] C. Pecharromán, F. E Betegón, J. F. Bartolomé, Sonia López-Esteban & José S. Moya; Adv. Mater. 2001, **13**, 20 (2001) 16.
[18] L. W. Matsch, Capacitors, Magnetic Circuits and Transformers, Prentice-Hall Inc, (1964)

[19] A. S. Sheik, R. W. Vest & G.M. Vest, IEEE Transactions on Ultrasonics, Ferroelectrics, and Frequency Control **36**, 4 (1989).
[20] J H Hannay, The Clausius-Mossotti equ: an alter. derivation; Eur I. Phls. **4** (1983) 141-143.
[21] H. Naceur, A. Megriche & Md El Maaoui; Orient. J. Chem. **29**, 3 (2013) 937-944.
[22] R. S. Devan, C. M. Kanamadi, S A Lokare & B K Chougule; Smart Mater. Struct. **15** (2006) 1877–1881.
[23] A. Lüker, Q. Zhang, P.B. Kirby, Ferroelectrics-Material aspects, First published July, 2011 Printed in Croatia, (2011).
[24] M. M. Vijatović, J. D. Bobić, B. D. Stojanović, Science of Sintering, **40** (2008) 235-244.
[25] S. Islam, A. Siddika, N. A Ahmed, N. Khatun, S. N. Rahman; A. Intl. Jour. of Res. in Sci., Tech., Eng. & Mathematics (AIJRSTEM) **13**, 1 (2016) 28-32.
[26] S.N. Rahman *et al.*, International Jour of Emerging Technologies in Computational and Applied Sciences(IJETCAS), **7**, 1 (2014) 5-19
[27] S. Mahboob, G Prasad & G S Kumar, Bulletin of Material Sci. **29**, 4 (2006) 347–355.